Electronic Supplementary Material (ESI) for Journal of Materials Chemistry C.

Supporting Information

Enhanced Photodetection Performance of Schottky $Pt/SnS_2/Al$ and $Au/SnS_2/Al$ Photodetectors

Supporting Information

Enhanced Photodetection Performance of Schottky $Pt/SnS_2/Al$ and $Au/SnS_2/Al$ Photodetectors

*Xia An,[1] Chao Fan, *[1,2] Xiancheng Meng,[1] Shuo Yuan,[1] Yongkai Jing,[1] Zhe Liu,[1] Chun Sun,[1] Yonghui Zhang,[1] Zihui Zhang,[1] Mengjun Wang,[1,2] Hongxing Zheng[1] and Erping Li[2]*

[1] State Key Laboratory of Reliability and Intelligence of Electrical Equipment, Hebei University of Technology, Tianjin, 300401, China.

[2]Zhejiang Provincial Key Laboratory of Advanced Microelectronic Intelligent Systems and Applications, Hangzhou, 310027, China.

Corresponding Authors

* fanch@hebut.edu.cn (C. Fan)

Contents list

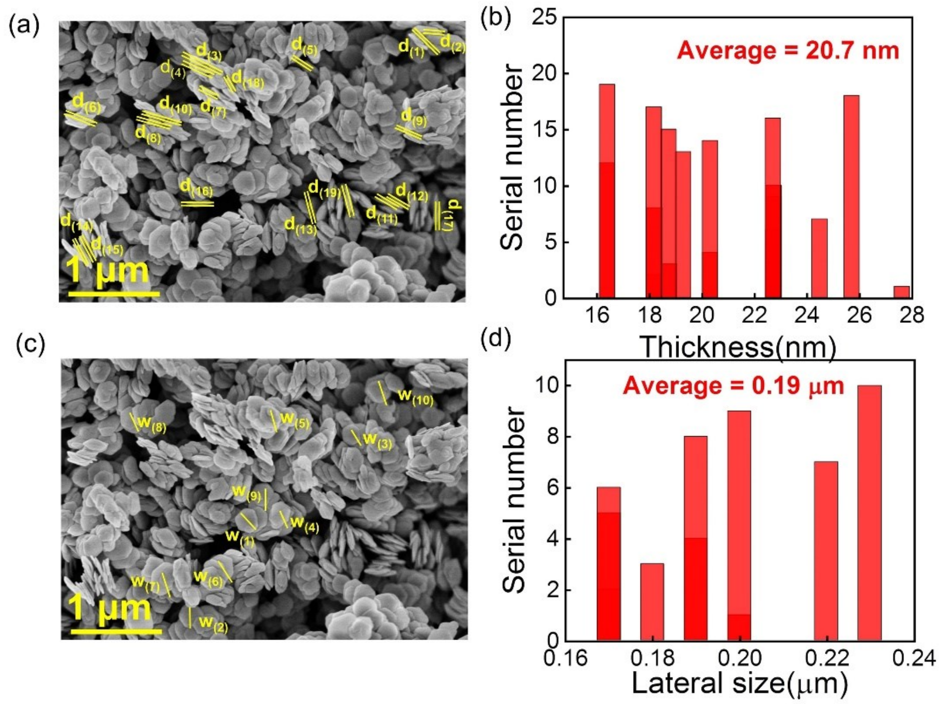

Fig S1. Thickness and lateral size of the SnS_2. (a) SEM image and (b) thickness statistical diagram of the as-synthesized SnS_2 nanosheets. (c) SEM image and (d) lateral size statistical diagram of the as-synthesized SnS_2 nanosheets.

The thickness was measured from the SEM image. A statistics analyze has been done and an average thickness of 20.7 nm was obtained. And an average lateral size of 0.19 μm has been obtained through a same statistical way.

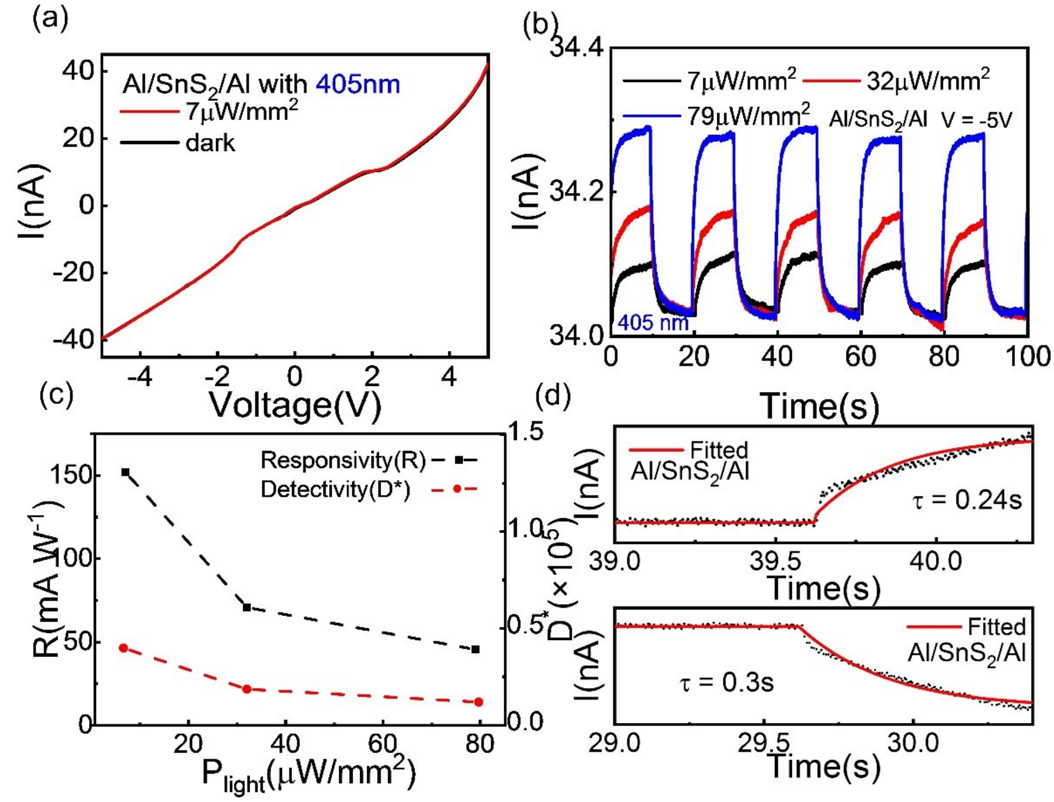

Fig S2. Characterization of the Ohmic Al/SnS_2/Al photodetector. (a) *I-V* characteristics in logarithmic coordinates and (b) temporal response of the photodetector. (c) Responsivity and detectivity of the photodetector. (d) Rise and (e) decay curves.

Fig S2a shows the current-voltage (*I-V*) curves of the Al/SnS_2/Al photodetector under illumination of a blue 405-nm laser with power intensities of 7 $\mu W \cdot mm^{-2}$ and in the dark. Fig S2b depicts the time-resolved photoresponse of the Al/SnS_2/Al photodetector. The current-time (*I-T*) cycles illustrate that the devices were stable and repeatable. The dark current is about 34.2 nA. When the light shined on the devices, the current increased till to saturation. Then as the light source was shut down, the current decreased to the original state. And current increased as the power intensity increased multiply.

For the Al/SnS_2/Al photodetector, at 7 $\mu W \cdot mm^{-2}$, R and D* are 152 $\mu A \cdot W^{-1}$ and 3.99×10^5, respectively. *R* and *D** decreased as power intensities increased as shown in Fig S2c, which illustrates the photodetector is more sensitive to weak signals. In Fig S2d, the rise and decay time are also two important parameters for a photodetector, reflect the speed of photoresponse. And the rise and decay edges were extracted from a single photoresponse cycle, and were fitted with two equations: $I = I_f + I_0 e^{-(t - t_0)/\tau_f}$ and $I = I_r - I_0 e^{-(t - t_0)/\tau_r}$. Thus, the rise and decay times are 0.24 and 0.3 s, respectively.

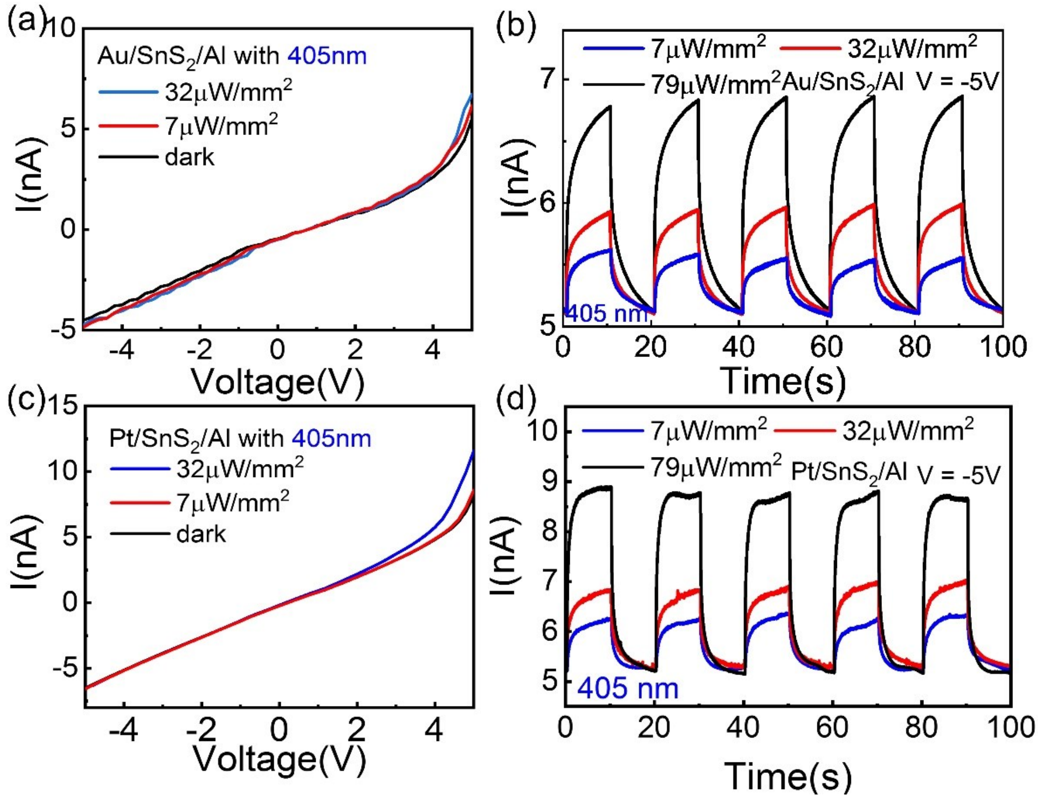

Fig S3. Photodetection performances of the Au/SnS_2/Al and Pt/SnS_2/Al photodetectors under illumination of a 405-nm laser. (a) *I-V* characteristics and (b) photoresponse of the Au/SnS_2/Al photodetector. (c) *I-V* characteristics and (d) photoresponse of the Pt/SnS_2/Al photodetector with different intensity and in the dark.

Fig S3a and c show their *I-V* curves that indicated significant Schottky contact under forward bias. The photoresponse of the Au/SnS_2/Al and Pt/SnS_2/Al photodetectors were measured under illumination with a green 532 nm laser of different power intensities, as shown in Fig S3b and d. SnS_2 photodetectors were operated in reverse bias, which is the reverse saturation state, and the external bias voltage was set as -5 V. Compared with the Al/SnS_2/Al photodetector, the curve shape is steeper and the dark current is reduced, which are more obvious on the Pt/SnS_2/Al photodetector and these devices also have good stability. It is apparent that the dark current of the photodetectors based on the Schottky contact were lower than that of the Al/SnS_2/Al photodetector.

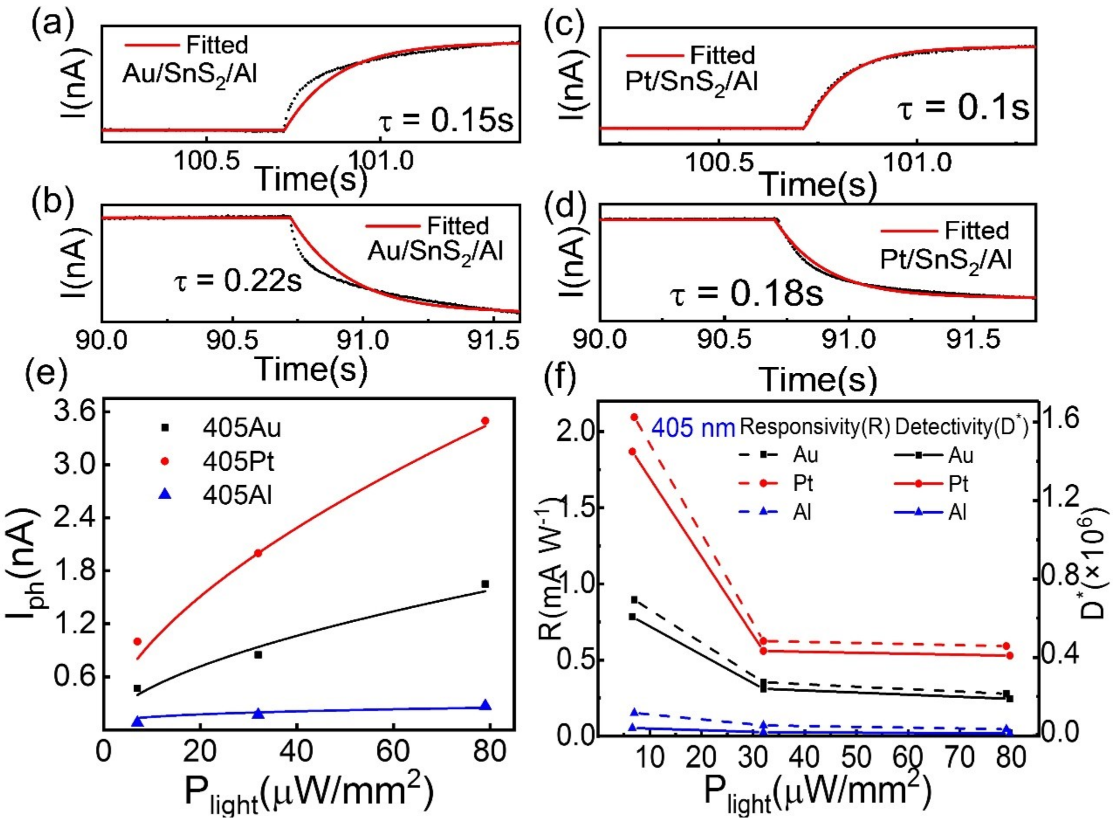

Fig S4. Performance comparison of the SnS_2-based photodetectors under illumination of a 405-nm laser. (a) Rise and (b) decay response of the Au/SnS_2/Al photodetector. (c) Rise and (d) decay time of the Pt/SnS_2/Al photodetector. (e) Photocurrent as function of the incident power intensity. (f) Responsivity and detectivity of the photodetectors.

Fig S4a-d show the rise and decay edges that are extracted and fitted. And the rise and decay time of the Au/SnS_2/Al photodetector are 0.15 s and 0.22 s, respectively. The Pt/SnS_2/Al photodetector are 0.1 s and 0.18 s, respectively. Fig S4e depicts the light response curves of Au, Al and Pt electrode photodetectors. As the incident light intensity increased, the photocurrent also increased, which indicates a positive relationship between the carrier photogeneration efficiency and the incident light absorption. The scatter plots were fitted with the equation $I_{\text{light}} = a P_{\text{light}}^{\alpha}$, where α reflects the photocurrent efficiency. The fit parameter values, α, were 0.27 for the Al/SnS_2/Al photodetector, 0.57 for the Au/SnS_2/Al photodetector, 0.61 for the Pt/SnS_2/Al photodetector. The values of α were all less than 1, which indicates that there was a loss of energy as the external light transformed into photocurrent due to trapping and recombination. The height values of Pt and Au electrode photodetectors indicate that they have better photoelectric conversion efficiency. As shown in Fig 4f, The R and $D*$ curves of the photodetectors under illumination of a green laser with different intensities were extracted. The *R* values of the Pt/SnS_2/Al, Au/SnS_2/Al and Al/SnS_2/Al photodetectors are 2.095 mA·W^{-1}, 895 μA·W^{-1} and 152 μA·W^{-1}, respectively. And the *D** values are 14.49×10^6 for the Pt/SnS_2/Al, 6.07×10^6 for the Au/SnS_2/Al, 3.99×10^5 for the Al/SnS_2/Al, respectively. *R* and *D** decreased with power intensities increased, showing that the Al/SnS_2/Al, Au/SnS_2/Al, and Pt/SnS_2/Al photodetectors are sensitive to weak signals. Table S1 shows the statistical data of photodetector performance under illumination of a 405-nm laser.

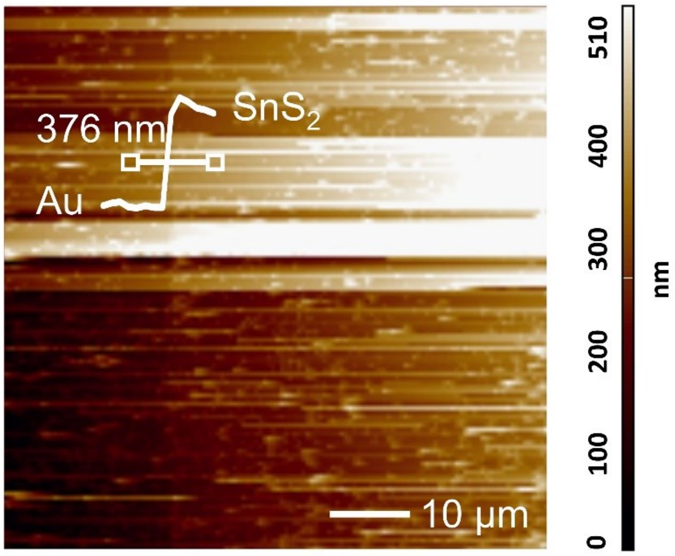

Fig. S5. AFM image of the SnS_2 nanosheets layer

The AFM images of the SnS_2 NSs layer of the Pt/SnS_2/Al photodetector are shown in Fig. S5. The thickness of the SnS_2 NSs layer was estimated to be 376 nm.

Tab. S1. Comparison of the photodetection performances of the three photodetectors under illumination of a 405-nm laser with an intensity of 7 μW/mm^2.

Photodetector 405 nm	R/μA·W^{-1}	D/Jones	Idark/nA	Response time/s (rise/decay)
Pt/SnS_2/Al	2095	14.49×10^6	4.9	0.1/0.18
Au/SnS_2/Al	895	6.07×10^6	5.1	0.15/0.22
Al/SnS_2/Al	152	3.99×10^5	34.2	0.24/0.3

Under illumination of a 405-nm laser, compared with the Ohmic Al/SnS_2/Al photodetector, the response times of the two Schottky Pt/SnS_2/Al and Au/SnS_2/Al photodetectors are shorter. The dark currents of the two Schottky photodetectors are about ten times lower than that of the Ohmic photodetector. And R and $D*$ of the two Schottky photodetectors are about ten times higher than that of the Ohmic photodetector as shown in Tab S1.